OPTIMAL DESIGN OF ENERGY CONVERSION UNITS AND ENVELOPES FOR RESIDENTIAL BUILDINGS

Thomas Schütz, Lutz Schiffer, Hassan Harb, Marcus Fuchs, and Dirk Müller
RWTH Aachen University, E.ON Energy Research Center
Institute for Energy Efficient Buildings and Indoor Climate
52074 Aachen, Germany
tschuetz@eonerc.rwth-aachen.de

ABSTRACT

The optimal design of buildings is a complex task involving energy systems as well as construction measures. Typically, in exact optimization models, only energy systems are considered, whereas envelope components are neglected. When considering both, heuristics are commonly used, which do not guarantee optimal or close to optimal results. Thus, this paper presents a building model that can be used in exact optimization problems for simultaneously considering energy systems and building envelopes. The developed model is based on ISO 13790 and verified according to ASHRAE 140 and further compared to a more detailed model. The findings show that the developed model fulfills the ASHRAE requirements for heating and cooling loads. The model computes similar heat demands as the more detailed model; however, cooling loads differ. Since our focus is on heating systems, the model is suitable for this application. The simultaneous optimization of energy system and envelope is further demonstrated for a residential building.

INTRODUCTION

The energy economic optimal design of buildings is a complex problem that involves buildings' electricity and heat consumption as well as generation and storage devices. According to Stadler et al. (2014), this problem is further complicated by the interrelationship between heat consumption, which is among other factors influenced by passive construction measures, and the building energy system (BES).

Most studies solely focusing on the optimal design of BES use exact optimization algorithms such as mixed integer linear programming (MILP). Since modelling buildings' heat transfer relationships often results in nonlinear equations, there have only been few attempts to include the design of building envelopes in MILP models. Instead, the simultaneous design of building envelopes and BES configurations commonly relies on heuristic approaches (Evins, 2014).

However, heuristics do neither guarantee optimal solutions, nor are they able to assess the quality of the incumbent solution (Floudas et al., 2009). This makes heuristics less preferable for optimization purposes if a global solution can be found. Therefore, the simultaneous integration of design decisions on buildings' envelopes and BES components presents a promising extension of known exact BES optimization models. In this manner, this paper presents the integration of a dynamic thermal building model in our previously developed BES optimization model.

The rest of this paper is structured as follows. The next section briefly summarizes existing studies on the integration of thermal building models and BES optimization with heuristic and exact methods. Afterwards, the building model used in this study and its implementation into the optimization model are presented. Subsequently, we present verification computations on our model based on technical standards and other, more detailed models. Next, the model is applied to design the optimal BES and envelope of a residential building. Finally, this paper closes with a summary and an outlook for future research.

LITERATURE REVIEW

Evins (2013) provides a recent review on optimization methods applied to building design. Most of the papers he analyzed combine classic building simulation programs such as EnergyPlus[1] or TRN-SYS[2] with heuristic optimization methods like Genetic Algorithms. The applications range from optimizing glazing and construction to determine plant capacities. The main benefits of this approach include reduced efforts for the optimization as most heuristic algorithms are publically available and high modelling accuracies of the building simulation programs. However, the usage of heuristics does not guarantee convergence towards a global optimum because the algorithm can get stuck in (low quality) local optima. Furthermore, heuristics do not provide a quality measure; therefore, it is not possible to assess how far away the incumbent solution could be from the global optimum. On the other hand, building simulation programs typically require huge effort for the parameterization and long computing times, which might be unnecessary at early planning stages.

Exact optimization algorithms offer a method that converges globally and provides an evaluation of the incumbent's solution quality at all times, making these algorithms a preferable choice. However, exact optimization algorithms typically rely on strict as-

[1] https://energyplus.net/
[2] http://www.trnsys.com/

sumptions like linearity or convexity which impede the modeling accuracy. Exact algorithms like MILP are used in academic applications for the optimal design and operation of BES, as illustrated by Mehleri et al. (2013) and Harb et al. (2015). In both works, buildings' thermal demands are considered as fixed time series that are computed before the optimization and only present parameters within the optimization.

Ashouri et al. (2013) include a low-order building model into the design and operation optimization of BES. This model is able to consider thermal masses for the BES components' operation. However, since this low-order model uses constant parameters, building envelopes optimizations cannot be conducted.

Asadi et al. (2012) implement a static model based on the Portuguese version of ISO 13790 to determine optimal building envelopes for retrofit purposes. They consider windows, insulation, roofs and solar collectors but their calculations are based on annual demands, therefore neglecting the BES components' operation and buildings' heat capacity.

Stadler et al. (2014) use a dynamic modeling approach to determine optimal investments in envelope components. This approach relies on an EnergyPlus simulation providing a basic heat demand profile from which demand reductions through investments in improved components are subtracted. This approach only allows for considering heat transmission but neglects radiation. Furthermore, buildings' heat capacity is also neglected.

In conclusion, there are only few studies simultaneously optimizing BES and envelopes which further rely on large simplifications in modeling the heat transfer processes. Therefore, this paper presents a method of including the hourly heat demand calculation described in ISO 13790 (2008) for optimizing buildings' envelopes and BES components at the same time.

MODELING

This section describes the existing BES optimization model without considering the building envelope, the chosen building model and its implementation into the optimization model.

BES optimization model

The BES optimization model extended in this paper is based on the authors' previous publications (Harb et al. 2015, Schütz et al. 2016); therefore, this section only provides a brief description. The model is formulated to design, size and schedule the operation of the BES of a single building, connected to an electricity and gas grid, at optimal costs. Figure 1 shows the structure of the model. Conventional heat generators such as boilers, combined heat and power (CHP) units, electrical heaters (EHs) and heat pumps (HPs) are considered. Furthermore, storage devices like electrical batteries (BATs) and thermal energy storage (TES) units are available. Solar generators like photovoltaic (PV) modules and solar thermal collectors (STCs) as well as peripheral devices like inverters are also included as possible parts of the optimal BES.

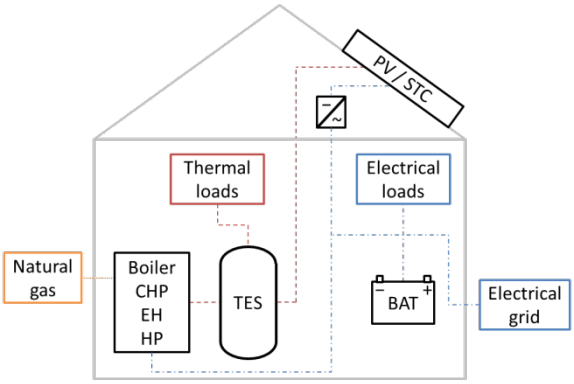

Figure 1 Building energy system structure

In the original model, the TES is the only link to the building's thermal demand. The corresponding energy balance is formulated similar to:

$$E_t = (1-k)\cdot E_{t-1} + \Delta t \cdot \left(\sum_g \phi_t^g - \phi_t^d\right) \qquad (1)$$

With E as the TES's stored energy, t the current time step, k the TES loss coefficient, Δt the time step length and ϕ_t^g and ϕ_t^d as heat generation and heat demand. The heat demand is the sum of space heating demand and domestic hot water usage. In the previous model, both were computed before the optimization was carried out. With this paper's approach, the demand for space heating is computed dynamically as part of the optimization.

Low-order building model

Figure 2 displays the low-order building model described in ISO 13790. The model lumps all components into one thermal mass with capacitance C_m and area A_m. Heat transfer from ventilation H_ve and through windows $H_\mathrm{tr,w}$ and opaque components $H_\mathrm{tr,op}$ are considered. Furthermore, three nodes model the indoor air temperature θ_air, the thermal capaci-

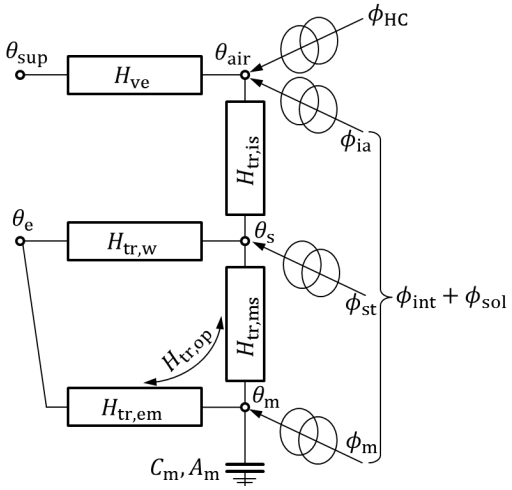

Figure 2 Low-order building model (ISO 13790)

tance's surface θ_s and mass temperature θ_m. Internal gains ϕ_{int} and solar gains ϕ_{sol} as well as the heating/cooling inputs ϕ_{HC} further affect these temperatures.

According to this ISO standard, the entire building is modeled as a single thermal zone since set temperatures typically do not differ by more than 4 K in residential buildings and because ventilation rates do not differ drastically between different rooms and also because the building is conditioned by a central heating system. Furthermore, shading, thermal bridges and windows' frame areas are neglected in our paper.

Building model implementation

The model requires weather inputs, such as solar irradiation on all outside surfaces and outside temperature. Additionally, a set of typical walls, windows, roofs, internal walls and ceilings as well as ground floor structures have to be provided. The optimization chooses the optimal combination from the set of provided types.

A set of binary variables x are used to model this decision process. x_{j,S_j} equals one if type S_j of component j is chosen and zero otherwise. Exactly one type of each component has to be chosen:

$$\sum_{s_j} x_{j,S_j} = 1 \tag{2}$$

Thermal mass

The thermal capacitance is computed as the sum of the product of each component's area and specific heat capacity:

$$C_m = \sum_{j,S_j} x_{j,S_j} \cdot \kappa_{j,S_j} \cdot A_j \tag{3}$$

ISO 13790 provides two methods for computing A_m. First, an algebraic method that introduces many nonlinear terms and secondly a simplified, table-based method. The table-based method classifies buildings as either very light, light, medium, heavy, or very heavy, with fixed upper and lower bounds $\left(f_{C,cl}^{ub} \text{ and } f_{C,cl}^{lb}\right)$ for each class. Accordingly, A_m is proportional $\left(f_{A,cl}\right)$ to the heated floor area A_f. Since the building's class is not known before the optimization and the algebraic method cannot be used within a linear context, we combine both approaches.

The thermal capacitance is computed as described before. The building's class z_{cl} immediately results from this capacitance and is chosen with the following two inequalities:

$$C_m \leq \sum_{cl} z_{cl} \cdot f_{C,cl}^{ub} \cdot A_f \tag{4}$$

$$C_m \geq \sum_{cl} z_{cl} \cdot f_{C,cl}^{lb} \cdot A_f \tag{5}$$

Afterwards, A_m results in

$$A_m = \sum_{cl} z_{cl} \cdot f_{A,cl} \cdot A_f \tag{6}$$

Heat transfer coefficients

$H_{tr,ms}$ describes the heat transfer between mass and surface nodes and is computed with:

$$H_{tr,ms} = 9.1 \frac{W}{m^2 \cdot K} \cdot A_m \tag{7}$$

The total opaque heat transfer coefficient is

$$H_{tr,op} = \sum_{j,S_j} b_{tr,j} \cdot x_{j,S_j} \cdot A_j \cdot U_{j,S_j} \tag{8}$$

The adjustment factor $b_{tr,j}$ is equal to $(\overline{\theta_{air}} - \bar{\theta}_e)/(\theta_{set} - \theta_e)$ for components with ground contact and one for the other. $\overline{\theta_{air}}$ and $\bar{\theta}_e$ are the annually averaged air and environment temperatures and θ_{set} is the thermal zone's set temperature.

$H_{tr,op}$ is split into a serial connection of $H_{tr,ms}$ and $H_{tr,em}$ which describes the heat transfer between mass and outdoor temperature. This formulation introduces a second nonlinearity that cannot be reformulated reasonably. Instead, we assume the numerical value of $H_{tr,ms}$ to be much bigger than that of $H_{tr,em}$. Consequently, $H_{tr,em}$ is approximated to be:

$$H_{tr,em} \approx H_{tr,op} \tag{9}$$

Heat transfer through windows is modeled with:

$$H_{tr,w} = \sum_{S_w} x_{w,S_w} \cdot A_w \cdot U_{w,S_w} \tag{10}$$

The heat transfer between surface and air node is:

$$H_{tr,is} = 3.45 \frac{W}{m^2 \cdot K} \cdot A_{tot} \tag{11}$$

A_{tot} describes the total internal surface area, which is the product of Λ_{at} (dimensionless ratio between internal surfaces and A_f) and A_f. According to the standard, a value of 4.5 is recommended for Λ_{at}.

Ventilation is modeled with:

$$H_{ve} = 1200 \frac{J}{m^3 \cdot K} \cdot q_{ve,avg} \tag{12}$$

$q_{ve,avg}$ stands for the time-average airflow rate.

Internal and solar gains

The internal gains, for example resulting from occupancy and electrical devices, can directly be computed. Solar gains on the other hand, depend on the chosen façade and windows. The general equation for solar gains through a component k is given with:

$$\phi_{sol,k} = A_{sol,k} \cdot I_{sol,k} - F_{r,k} \cdot \phi_{r,k} \tag{13}$$

$A_{sol,k}$ is the effective area of component k, which results in $A_{sol,k} = A_k \cdot 0.9 \cdot g_{gl,n}$ for windows and $A_{sol,k} = A_k \cdot U_k \cdot \alpha_S \cdot R_{se}$ for opaque components. $g_{gl,n}$ describes the solar energy transmittance for radiation perpendicular to the glazing, α_S the surface's absorption coefficient and R_{se} the external surface heat resistance. The solar radiation onto a tilted surface $I_{sol,k}$ is computed as the sum of direct, diffuse and reflected radiation, and depends on weather and geometric influences. The direct and reflected parts are computed as described in (Duffie et al., 2013) and the influence of diffuse radiation is assessed with the approach presented in

(Perez et al., 1990). The form factor $F_{\mathrm{r},k}$ between component and sky is 1 for unshaded horizontal roofs and 0.5 for unshaded vertical walls. $\phi_{\mathrm{r},k}$ stands for the thermal radiation to the sky and is calculated as $\phi_{\mathrm{r},k} = A_k \cdot U_k \cdot R_{\mathrm{se}} \cdot 5 \cdot \varepsilon \cdot 11\ \frac{\mathrm{W}}{\mathrm{m}^2}$, with ε being the external surface's emissivity for thermal radiation.
Internal and solar gains are distributed to the three temperature nodes. The heat flow directly affecting the air node ϕ_{ia} is equal to half of the internal gains.

$$\phi_{\mathrm{ia}} = 0.5 \cdot \phi_{\mathrm{int}} \tag{14}$$

The heat flow into the thermal mass ϕ_{m} is:

$$\phi_{\mathrm{m}} = \frac{A_{\mathrm{m}}}{A_{\mathrm{tot}}} \cdot 0.5 \cdot \phi_{\mathrm{int}} + \frac{A_{\mathrm{f}}}{A_{\mathrm{tot}}} \cdot \sum \left(h_{cl,j,S_j} \cdot f_{A,cl} \cdot \phi_{\mathrm{sol},j,S_j,k} \right) \tag{15}$$

In this equation, h_{cl,j,S_j} represents the nonlinear product $z_{cl} \cdot x_{j,S_j}$. Since both factors are binary variables, h_{cl,j,S_j} is binary, too. This expression can be linearized without loss of accuracy, by introducing the following three constraints:

$$h_{cl,j,S_j} \leq z_{cl} \tag{16}$$

$$h_{cl,j,S_j} \leq x_{j,S_j} \tag{17}$$

$$h_{cl,j,S_j} \geq z_{cl} + x_{j,S_j} - 1 \tag{18}$$

The heat flow onto the thermal mass's surface ϕ_{st} is:

$$\phi_{\mathrm{st}} = \phi_1 - \phi_2 + \phi_{\mathrm{sol}} - \phi_{\mathrm{m}} \tag{19}$$

Where ϕ_1 and ϕ_2 are abbreviations for

$$\phi_1 = \left(\frac{1}{2} - \frac{0.5 \cdot A_{\mathrm{w}}}{9.1 \cdot A_{\mathrm{tot}}} \cdot \sum \left[x_{w,S_w} \cdot U_{w,S_w} \right] \right) \cdot \phi_{\mathrm{int}} \tag{20}$$

$$\phi_2 = \frac{A_{\mathrm{w}}}{9.1 \cdot A_{\mathrm{tot}}} \cdot \sum \left[h_{w,S_w,j,S_j} \cdot U_{w,S_w} \cdot \phi_{\mathrm{sol},j,S_j,k} \right] \tag{21}$$

h_{w,S_w,j,S_j} represents the product of x_{w,S_w} and x_{j,S_j} and is constrained similarly to h_{cl,j,S_j}.

Linearized building model

The energy balances of the building model shown in Figure 2, can be formulated as three linear equations:

$$H_{\mathrm{tr,ms}} \cdot (\theta_{\mathrm{m}} - \theta_{\mathrm{s}}) + H_{\mathrm{tr,em}} \cdot (\theta_{\mathrm{m}} - \theta_{\mathrm{e}}) = \phi_{\mathrm{m}} - C_{\mathrm{m}} \cdot \frac{\partial \theta_{\mathrm{m}}}{\partial t} \tag{22}$$

$$H_{\mathrm{tr,ms}} \cdot (\theta_{\mathrm{s}} - \theta_{\mathrm{m}}) + H_{\mathrm{tr,is}} \cdot (\theta_{\mathrm{s}} - \theta_{\mathrm{air}}) + H_{\mathrm{tr,w}} \cdot (\theta_{\mathrm{s}} - \theta_{\mathrm{e}}) = \phi_{\mathrm{st}} \tag{23}$$

$$H_{\mathrm{ve}} \cdot (\theta_{\mathrm{air}} - \theta_{\mathrm{sup}}) + H_{\mathrm{tr,is}} \cdot (\theta_{\mathrm{air}} - \theta_{\mathrm{s}}) = \phi_{\mathrm{ia}} + \phi_{\mathrm{HC}} \tag{24}$$

All products of any H_{tr}-value and a node's temperature (θ_{air}, θ_{s} and θ_{m}) have to be further linearized. Since all H_{tr}-values can be expressed as a product of a binary decision variable and a set of given parameters, the product of H_{tr} and θ can be linearized without loss of accuracy. Exemplarily, this linearization is explained for $H_{\mathrm{tr,ms}} \cdot \theta_{\mathrm{m}}$:

$$H_{\mathrm{tr,ms}} \cdot \theta_{\mathrm{m}} = 9.1 \frac{\mathrm{W}}{\mathrm{m}^2 \cdot \mathrm{K}} \cdot \sum_{cl} z_{cl} \cdot \theta_{\mathrm{m}} \cdot f_{A,cl} \cdot A_{\mathrm{f}} \tag{25}$$

The nonlinear product of z_{cl} and θ_{m} is replaced with a new variable $\xi_{cl,\mathrm{m}}$ that is further constrained with:

$$z_{cl} \cdot \theta_{\mathrm{m}}^{\mathrm{lb}} \leq \xi_{cl,\mathrm{m}} \leq z_{cl} \cdot \theta_{\mathrm{m}}^{\mathrm{ub}} \tag{26}$$

$$(1 - z_{cl}) \cdot \theta_{\mathrm{m}}^{\mathrm{lb}} \leq \theta_{\mathrm{m}} - \xi_{cl,\mathrm{m}} \leq (1 - z_{cl}) \cdot \theta_{\mathrm{m}}^{\mathrm{ub}} \tag{27}$$

$\theta_{\mathrm{m}}^{\mathrm{lb}}$ and $\theta_{\mathrm{m}}^{\mathrm{ub}}$ represent lower and upper bounds for θ_{m} – in our case 0 °C and 50 °C. Equations (26) ensure that $\xi_{cl,\mathrm{m}}$ is equal to zero if z_{cl} is zero. Equations (27) force $\xi_{cl,\mathrm{m}}$ to be equal to θ_{m} if z_{cl} is one.
The partial derivative $C_{\mathrm{m}} \cdot \frac{\partial \theta_{\mathrm{m}}}{\partial t}$ in equation (22) is approximated with $C_{\mathrm{m}} \cdot \frac{\theta_{\mathrm{m},t} - \theta_{\mathrm{m},t-1}}{\Delta t}$, where $\theta_{\mathrm{m},t}$ denotes θ_{m} at time step t and $\theta_{\mathrm{m},t-1}$ at the previous time step. The products of C_{m} and θ_{m} are treated in the same manner as the products of H and θ.
Finally, we ensure that the air temperature is always above a lower bound to guarantee thermal comfort. Since no cooling system is investigated, an upper bound is not explicitly formulated, but since heating leads to additional costs, the optimization does not overheat the building.

$$\theta_{\mathrm{air}} \geq \theta_{\mathrm{set}}^{\mathrm{lb}} \tag{28}$$

Design heat load

In order to appropriately size BES components, a design heat load based on DIN EN 12831 (2003), considering chosen building elements is computed:

$$\phi_{\mathrm{HC}}^{\mathrm{DHL}} = \left(\sum_{j,S_j} \left[\tilde{b}_{\mathrm{tr},j} \cdot x_{j,S_j} \cdot A_{j,S_j} \cdot U_{j,S_j} \right] + 1200\ \frac{\mathrm{J}}{\mathrm{m}^3 \mathrm{K}} \cdot V \cdot n \right) \cdot (\theta_{\mathrm{set}}^{\mathrm{DHL}} - \theta_{\mathrm{e}}^{\mathrm{DHL}}) \tag{29}$$

$\tilde{b}_{\mathrm{tr},j}$ describes the adjustment factor which is $1.45 \cdot b_{\mathrm{tr},j}$ for ground floors and 1 otherwise. V and n are the building's volume and air exchange rate. $\theta_{\mathrm{set}}^{\mathrm{DHL}}$ and $\theta_{\mathrm{e}}^{\mathrm{DHL}}$ stand for the nominal indoor set temperature and nominal outdoor temperature.

VERIFICATION

ISO 13790 is mainly intended for estimating annual energy demands for space heating and cooling. This section illustrates that both our implementation of this guideline as well as the linearized model suitable for MILP optimization purposes, are able to accurately compute annual and hourly heating and cooling loads. The verification consists of the ASHRAE guideline 140 which provides a generic test case, and a second comparison with a more detailed low-order model for a typical residential building.

ASHRAE 140

ASHRAE standard 140 (ASHRAE 140, 2011) provides a full set of test procedures for building energy analysis computer programs. Our verification however is restricted to the so called "Class I test procedures" for "Building Thermal Envelope and Fabric Load Basic Tests". These tests are divided into low

mass, high mass and free float tests. All test cases are derived from test case 600, which describes a single zone building located in Denver, Colorado, with two windows facing south and an adiabatic ground floor. Cases 620, 640 and 650 vary the windows' positions, thermostat's set points and ventilation rates. While cases 600, 620, 640, and 650 describe a building with a low thermal mass, cases 900, 920, 940, and 950 model a heavy thermal mass. Cases 610, 630, 910, 930 and 960 are omitted because they require shading effects or a second thermal zone, which is currently beyond the scope of the presented model.

The main differences between the original ISO 13790 model and the simplified model suitable for MILP optimization purposes are the computation of A_m and $H_\mathrm{tr,em}$. Table 1 shows that for case 600, A_m is 12% smaller in the simplified model than in the original one. Consequently, $H_\mathrm{tr,ms}$ is also reduced by 12%. However, the effect on $H_\mathrm{tr,em}$ is only 4%. As $H_\mathrm{tr,em}$ is smaller in the simplified model, the building's thermal insulation is slightly overestimated.

Table 1 Parameters ASHRAE 140, light mass cases

	A_m in m²	$H_\mathrm{tr,ms}$ in W/K	$H_\mathrm{tr,op}$ in W/K	$H_\mathrm{tr,em}$ in W/K
ISO (simpl.)	120.0	1092.0	49.1	49.1
ISO (orig.)	137.0	1246.4	49.1	51.1

The annual heating and cooling demands are summarized in Figure 3. Positive values stand for heating demands and negative values for cooling demands. The simplified and original implementations yield very similar results, which are moreover within the ASHRAE guideline's reference results obtained with standard building energy simulation programs.

Hourly heating and cooling loads for January 4th are shown in Figure 4. The computed loads are slightly below the minimum reference results between hours 9 and 11 that are given in ASHRAE 140. The maximum deviation is 0.175 kW in the original implementation and 0.230 kW in the simplified one. The maximum deviation between both models is 0.117 kW and the average deviation is 0.063 kW.

Table 2 illustrates that the implemented simplifications affect the heavy mass building in a similar magnitude as the light mass building. However, in the light mass building, A_m was 12% underestimated, whereas in the heavy mass building, A_m is approx. 22% overestimated. The assumption of $H_\mathrm{tr,ms}$ being much bigger than $H_\mathrm{tr,op}$ proves to be justified, even if the approximation of A_m is inaccurate.

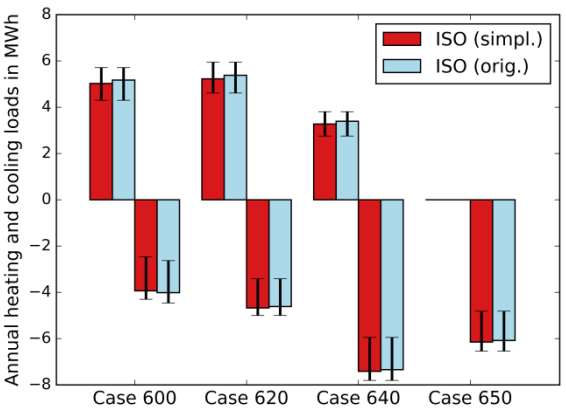

Figure 3 Annual loads, light mass cases

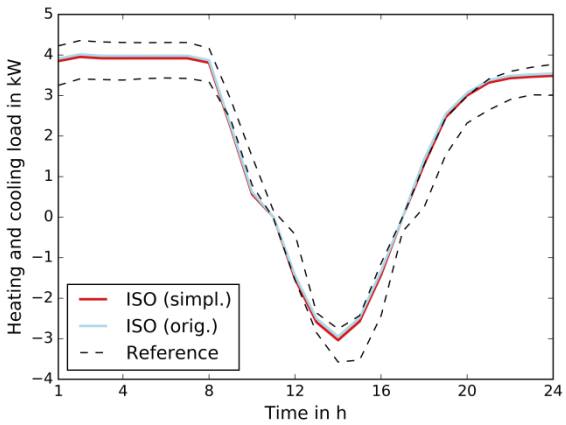

Figure 4 Hourly loads on January 4th, case 600

Table 2 Parameters ASHRAE 140, heavy mass cases

	A_m in m²	$H_\mathrm{tr,ms}$ in W/K	$H_\mathrm{tr,op}$ in W/K	$H_\mathrm{tr,em}$ in W/K
ISO (simpl.)	144.0	1310.4	49.0	49.0
ISO (orig.)	117.9	1073.2	49.0	51.3

Similarly, the annual heating and cooling loads are shown in Figure 5. The findings again prove that our implementations are within the reference results and therefore fulfill the requirements of ASHRAE 140.

The hourly loads for test case 900 on January 4th are presented in Figure 6. This plot shows that for the heavy mass building, both models comply with the reference solutions at all times. Though, the deviation between both models increases compared with the light mass cases. The maximum deviation between both models is 0.364 kW and the average deviation is 0.133 kW.

The free float cases, in which the internal heating system is deactivated, as well as the analysis of the peak demands are not included in this paper due to space limitations. Both reinforce that the introduced simplifications only lead to minor differences in the results. Furthermore, the results reveal that our im-

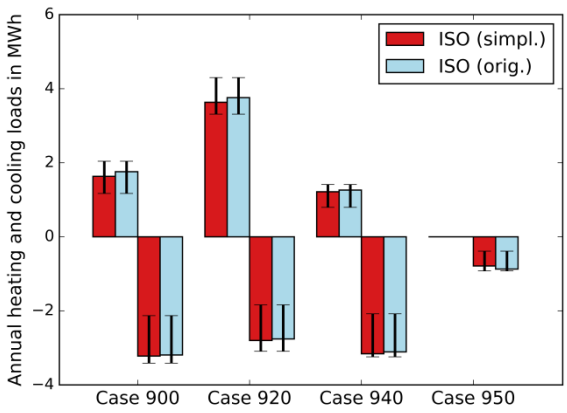

Figure 5 Annual loads, heavy mass cases

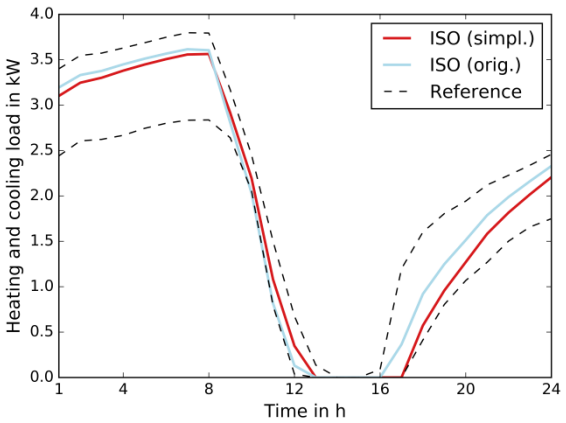

Figure 6 Hourly loads on January 4th, case 900

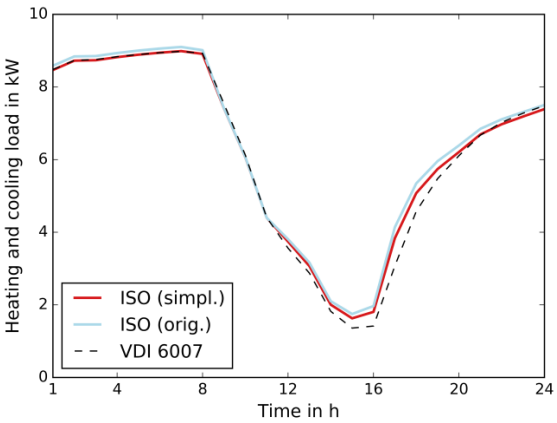

Figure 7 Hourly loads on January 4th, light mass

plementations are suitable for assessing the thermal behavior of the ASHRAE building.

Improved low-order model

Our implementations are further compared with an improved low-order model developed by Lauster et al. (2014)[3] based on the German engineering guideline VDI 6007 (2015). In contrast to the ISO 13790 standard, this guideline has been developed for assessing hourly loads. Since this model introduces more nonlinearities than the ISO model, we chose the ISO model for our optimization problem. The comparison with the improved low-order model serves for evaluating the suitability of our implementation for a more realistic example, since the modelled building is more representative than the ASHRAE building and further effects such as ground contact can be considered.

The building considered for this comparison is a two-story building with a heated floor area of 150 m² and each story has a height of 3 m. Each outside wall has an area of 34.75 m² and a window area of 7.5 m². Ground floor and flat roof are 99.75 m² large. Ceiling and inner walls account for 75 m² and 375 m². The air exchange rate is set to 0.5 h^{-1}.

The comparison again includes a light construction building and a heavy mass construction. The effects of our simplifications on A_m and $H_\mathrm{tr,em}$ are shown in Table 3 for the light mass building. While A_m and consequently $H_\mathrm{tr,ms}$ are overestimated by 11.4%, $H_\mathrm{tr,em}$ is only reduced by 3.5%.

Table 3 Parameters comparison, light mass

	A_m in m²	$H_\mathrm{tr,ms}$ in W/K	$H_\mathrm{tr,op}$ in W/K	$H_\mathrm{tr,em}$ in W/K
ISO (simpl.)	375.0	3412.5	108.0	108.0
ISO (orig.)	336.6	3062.6	108.0	111.9

For comparing the hourly loads, January 4th has been chosen again. The hourly loads in this day are depicted in Figure 7. The maximum difference between simplified and original ISO model is 0.3 kW and between the simplified ISO model and the VDI model 0.8 kW with an average value of 0.1 kW.

Table 4 illustrates that the simplifications again heavily affect A_m and $H_\mathrm{tr,em}$, leading to deviations of 19.3%. However, $H_\mathrm{tr,em}$ is again estimated accurately with a deviation of only 2.2%.

Table 4 Parameters comparison, heavy mass

	A_m in m²	$H_\mathrm{tr,ms}$ in W/K	$H_\mathrm{tr,op}$ in W/K	$H_\mathrm{tr,em}$ in W/K
ISO (simpl.)	525.0	4777.5	131.0	131.0
ISO (orig.)	650.4	5918.2	131.0	133.9

The differences in the hourly heating loads of the heavy construction are more distinct as shown in Figure 8. The maximum deviation of simplified and original ISO model is 0.6 kW. The VDI model and the simplified ISO model differ by maximum 0.5 kW and on average by 0.3 kW for this day.

The annual heating and cooling loads for this comparison are shown in Figure 9. The annual demands for heating of all three models agree well, while the cooling demands are significantly larger in the ISO models. The simplified model leads to marginally bigger deviations from the VDI model than the original ISO implementation, but the deviation is only 3.1% for the heating and 3.7% for the cooling demands. The deviation between simplified model and VDI model is 4.9% for the heating and 40.7% for the

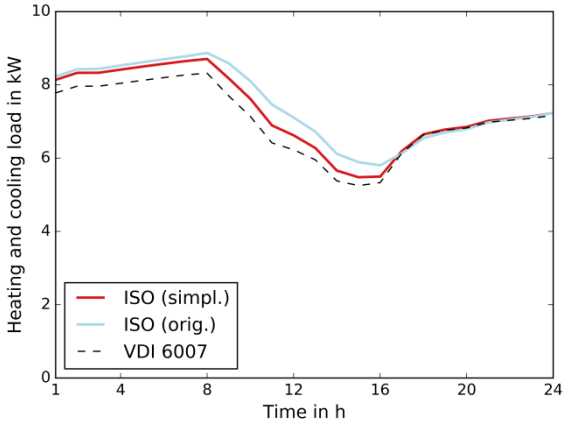

Figure 8 Hourly loads on January 4th, heavy mass

[3] The building models including documentation and examples are publically available at https://github.com/RWTH-EBC/AixLib.

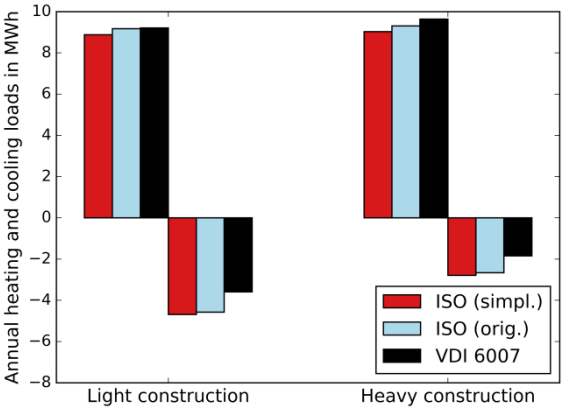

Figure 9 Annual heating and cooling loads

cooling demands. This large relative deviation in the cooling demand however is due to the low absolute demands which increase the relative differences. Furthermore, these differences are due to the modeling of ground contact which is based on a pre-defined indoor set-temperature that is different from the actual temperature resulting in the simulations.

Summary

The ASHRAE verification and comparison with the VDI model illustrate that the introduced simplifications barely affect the results of the model. In fact, both show that our implementations are able to accurately compute the total annual heating demands. The deviations in the cooling demands are significantly larger than for the heating demands, but since cooling systems are currently not considered in our BES optimization, deviations in the cooling demands are negligible. The hourly heating and cooling loads are further predicted very accurately with the implementation for light construction buildings, whereas there are noticeable deviations for heavy construction buildings. However, these deviations are within the feasible range of reference results provided in ASHRAE 140.

Overall, the simplified model has been shown to be suitable for modeling building physics in our BES optimization context.

SCENARIO

The coupled BES and envelope optimization is applied to the residential building used in the comparison with the improved low-order model. Table 5 summarizes the considered typical opaque building components from which the optimizer can choose. We consider three different types of outside walls and two types of roofs, ground floor constructions, internal walls and drop ceilings/floors. Index 1 always represents the heaviest and typically most expensive option while the highest index (2, resp. 3) stands for the lightest and typically cheapest construction.

Table 6 lists the available windows which describe a triple (1) and a double (2) insulation glazing. All components comply with the minimum requirements

Table 5 Opaque building components

Component (j)	S_j	κ kJ/(m²K)	U W/(m²K)	inv €/m²
Outside wall	1	58.29	0.177	73.65
	2	49.09	0.238	70.34
	3	11.25	0.236	38.06
Roof	1	55.00	0.191	103.70
	2	11.25	0.190	70.75
Ground floor	1	158.00	0.190	56.29
	2	138.00	0.320	48.72
Internal wall	1	45.36	-	28.23
	2	11.25	-	11.20
Drop ceiling and floor	1	80.00 200.00	-	36.23
	2	0.00 100.07	-	45.80

Table 6 Windows

S_j	U W/(m²K)	g_{gl} w/o unit	ε w/o unit	inv €/m²
1	0.544	0.500	0.9	371.00
2	0.927	0.575	0.9	320.00

for German residential buildings according to the German Energy Saving Ordinance EnEV 2014.

The optimal combination of considered envelope components is shown in Table 7. The presented investment costs are annualized for a considered time period of 10 years. The chosen components are mostly the cheapest available types with the lowest thermal capacity and highest (worst) U-values. This suggests that current standards provided by EnEV 2014 might exceed optimality from an economic perspective. The corresponding BES consists of the smallest considered gas boiler and thermal storage tank, whereas the available area for PV is fully utilized. The total annualized costs of BES and building envelope amount to 4094.33 €, from which roughly 72% are due to envelope components and 28% to BES equipment and operation.

Table 7 Optimal envelope components

Component (j)	S_j	$\kappa \cdot A$ MJ/K	$U \cdot A$ W/K	inv €
Outside wall	3	1.901	39.957	569.61
Roof	2	1.122	18.919	624.97
Ground floor	2	13.766	31.947	430.37
Internal wall	2	4.219	-	185.97
Drop ceiling and floor	2	7.505	-	304.20
Window	2	-	27.804	850.14
Sum		28.513	118.627	2965.26

CONCLUSION

This paper presents a simplified version of ISO 13790 that can be used in exact optimization models to simultaneously choose and dimension building envelope and BES components. Therefore, synergies between both can be utilized. The model has been verified according to ASHRAE 140 and

compared to a more detailed low-order building model. The results of this verification indicate that our simplifications only marginally affect the model's accuracy compared with the original ISO model. Furthermore, the simplified model has been confirmed to accurately predict annual heating loads and the general behavior of hourly heating and cooling loads. Deviations regarding annual cooling loads compared with the more detailed model occurred, but these can be neglected for our application which only considers heating systems.

Future works include increasing the model's accuracy by for example considering multiple thermal zones, and applying the model to different buildings for further assessing governmental regulations for German residential buildings.

NOMENCLATURE

A,	area;
C,	capacity;
E,	storage energy content;
F,	form factor;
H,	heat transfer coefficient;
I,	solar irradiation;
R_{se},	external surface heat resistance;
U,	thermal transmittance;
V,	volume;
$b_{\mathrm{tr},j}$,	adjustment factor;
f,	empirical factors;
g,	total solar energy transmittance;
h,	linearized product of two binary variables;
k,	storage loss coefficient;
n,	air exchange rate;
$q_{\mathrm{ve,avg}}$,	time-average airflow rate;
x_{j,S_j},	decision if type S_j of component j is installed (binary variable);
Δt,	time step length;
z,	building's class (binary variable).
α,	absorption coefficient;
ε,	emissivity for thermal radiation;
θ,	temperature;
κ,	specific heat capacity;
ξ,	linearized product of binary and continuous variables;
ϕ,	heat flow rate.

ACKNOWLEDGEMENT

This work was supported by the Helmholtz Association under the Joint Initiative "Energy System 2050 – A Contribution of the Research Field Energy".

REFERENCES

Asadi, E., Gameiro da Silva, M., Henggeler Antunes, C., Dias, L. 2012. Multi-objective optimization for building retrofit strategies: A model and an application. Energy and Buildings (44):81-87.

Ashouri, A., Fux, S.S., Benz, M.J., Guzzella, L. 2013. Optimal design and operation of building services using mixed-integer linear programming techniques. Energy (59):365-376.

ASHRAE (American Society of Heating, Refrigerating and Air-Conditioning Engineers). 2011. ASHRAE 140: Standard Method of Test for the Evaluation of Building Energy Analysis Computer Programs.

DIN (Deutsches Institut für Normung – engl. German Institute for Standardization). 2003. DIN EN 12831: Heating systems in buildings - Method for calculation of the design heat load.

Duffie, J.A., Beckman, W.A. 2013. Solar Engineering of Thermal Processes. John Wiley & Sons, Inc., Hoboken, New Jersey.

Evins, R. 2013. A review of computational optimisation methods applied to sustainable building design. Renewable and Sustainable Energy Reviews (22):230-245.

Floudas, C.A., Pardalos, P.M. 2009. Encyclopedia of Optimization. Springer Science+Business Media

Harb, H., Reinhardt, J., Streblow, R., Müller, D. 2015. MIP approach for designing heating systems in residential buildings and neighbourhoods. Journal of Building Performance Simulation.

ISO (International Organization for Standardization). 2008. ISO 13790: Energy performance of buildings - Calculation of energy use for space heating and cooling.

Lauster, M., Teichmann, J., Fuchs, M., Streblow, R., Müller, D. 2014. Low order thermal network models for dynamic simulations of buildings on city district scale. Build. Environ. (73):223-231.

Mehleri, E.D., Sarimveis, H., Markatos, N.C., Papageorgiou, L.G. 2013. Optimal design and operation of distributed energy systems: Application to Greek residential sector. Renewable Energy (51):331-342.

Perez, R., Ineichen, P., Seals, R., Michalsky J., Steward, R. 1990. Modeling daylight availability and irradiance components from direct and global irradiance. Solar Energy (44):271-289.

Schütz, T., Harb, H., Fuchs, M., Müller, D., Optimal Design of Building Energy Systems for Residential Buildings. 12th REHVA World Congress CLIMA 2016; 2016 May 22-25; Aalborg, Denmark.

Stadler, M., Groissböck, M., Cardoso, G., Marnay, C. 2014. Optimizing Distributed Energy Resources and building retrofits with the strategic DER-CAModel. Applied Energy (132):557-567.

VDI (Verein Deutscher Ingenieure – engl. Association of German Engineers). 2015. VDI 6007: Calculation of transient thermal response of rooms and buildings.